Trabeculae microstructure parameters serve as effective predictors for marginal bone loss of dental implant in the mandible

Hengguo Zhang
Nanjing Medical University
Jie Shan
nanjing medical university
Ping Zhang
nanjing medical university
Hongbing Jiang (jhb@njmu.edu.cn)
nanjing medical university https://orcid.org/0000-0002-3748-0381

Research article

Keywords: Trabecular bone, marginal bone loss, Radiology, Imaging, Statistics

Posted Date: January 17th, 2020

DOI: https://doi.org/10.21203/rs.2.21166/v1

Abstract

Background : To investigate the effectiveness and feasibility of machine learning models based on trabecular microstructure parameters for predicting the occurrence of marginal bone loss (MBL) of the submerged dental implant in mandible.

Methods : Clinical variables and morphological parameters of trabecular bone were collected from 81 subjects with submerged implants in the mandible (41 cases of abnormal MBL and 40 as normal controls). We measured the peri-implant MBL level by a cone-beam computed tomography (CBCT) at the follow-up of 20.95±2.67 months after functional loading. The morphological parameters and possible factors associated with MBL were collected in a mean of 3.98±1.06 months at the early loading stage. All variables were analyzed using correlation and covariance matrices. Support vector machine (SVM), artificial neural network (ANN), logistic regression (LR) model and random forest (RF) were actualized to predict abnormal MBL.

Results : At the early stage of functional loading, the abnormal MBL cases showed a significant increase of structure model index (SMI) and trabecular pattern factor (Tb.Pf) in peri-implant. Meanwhile, SMI and Tb.Pf simultaneously revealed a significantly high positive correlation with MBL. The LR model exhibited the best outcome in predicting MBL (AUC = 0.956), followed by SVM (AUC = 0.928), RF (AUC = 0.917), ANN (AUC = 0.900), SMI alone (AUC = 0.705) and Tb.Pf alone (AUC = 0.663). Compared with one single predictor, all algorithm models yielded significantly superior performance.

Conclusion : Abnormal MBL cases demonstrated the premonitory morphological variation in trabecular bone at the early stage. MBL prediction could be achieved by machine learning methods.

1. Background

Peri-implant bone tissue is fundamental for the initial stability and long-term survival of dental implants, and marginal bone resorption around the implant could result in implant failure.[1, 2] Radiographic assessment of marginal bone loss (MBL) was invariably considered as an authoritative criterion to evaluate implant success.[3, 4] Currently, acceptable standards of implant success are as follows: less than 1.5-2.0 mm MBL after the first year of functional loading, and after that less than 0.2 mm annually.[3, 5, 6] The above criteria provide explicit cut-off rules, MBL often cannot be avoided. To prevent severe MBL, it is important to find accurately predictors for MBL.

Surgical implant placement and functional prosthesis usually accompany with continuous bone loss and formation.[7] At the early post-loading stage, occlusal force transmits through the implant to the alveolar bone and promotes bone remolding. Due to its obviously lower mean elastic moduli and hardness, trabecular bone has a more efficient response and adaption to the biomechanics effect than cortical bone.[8] The morphological and mechanical properties of trabecular bone in this process can be exhibited by more than twenty morphology parameters. Other factors that might impact bone remolding or MBL include the configuration of dental implant,[9, 10] cortical bone thickness,[11] periodontal disease

susceptibility,[12] and smoking[13]. However, most of these predictive models are based on traditional statistical methods in which the patient populations were small and the risk factors were manually selected by experts. Therefore, over- or under-fitting or misattribution of error rates might exist. Hence, the establishment of a precise model to predict bone remodeling or MBL is still a challenging exploration.

As a branch of artificial intelligence, machine learning utilizes statistical and optimization techniques to learn and detect in-depth relationships from complex medical data.[14] The establishment of machine learning models can identify and classify the relative importance of the variables. Machine learning has been gradually adopted to predict the progression of disease.[15, 16] To the best of our knowledge, using machine learning to predict MBL has rarely appeared in published studies.

Hence, the purposes of the study were as follows: (a) to identify how to collect and analyze the morphological parameters, (b) to explore the correlation between all variables and identify the most precise predictors of MBL, (c) to establish and verify each machine learning algorithm that predicts MBL occurrence.

2. Methods

2.1. Patients

All subjects received implant treatment between January 2016 and March 2019 in the Department of Oral and Maxillofacial Surgery of Affiliated Stomatological Hospital of Nanjing Medical University were screened. All procedures performed in studies were in accordance with the ethical standards of the Affiliated Stomatological Hospital of Nanjing Medical University (Approval number: PJ2019-038-001). Before the dental implant surgery, all patients provided written informed consent.

The inclusion criteria of subjects were as follows: above 18 years of age with good health; having received fixed prosthesis of mandibular implant; at least one year after loading; available integrated clinical data; valid cone-beam computed tomography (CBCT) examination conducted at the following three time-points: (T_1) immediately after the final prosthesis, (T_2) at the follow-up between three months and six months after loading, and (T_3) at the follow-up above one year of post-loading. Patients diagnosed with clinical or absolute failure based on the current guideline [5] were excluded. Patients with an incomplete periodontal follow-up examination and treatment record were also excluded. Patients with smoking cessation for more than three months before surgical implant placement were taken as non-smokers. Patients who had received bone augmentation were excluded. A retrospective review of the medical records was conducted to obtain the characteristics and radiographic data.

2.2. Measurement of MBL

All subjects were examined by the CBCT (NewTom 5G cone-beam computed tomography device, Verona, Italy) at a resolution of 200 dpi at the three time-points. The original radiographs were reconstructed using the center of the implant in the sagittal, coronal, and transverse plane. The implant diameter was

used to calibrate the reconstructed images. MBL measurement was performed as follows: the horizontal interface between implant and abutment was validated as the reference loci; vertical distances from the loci to the most coronal level of bone to implant contact at the mesial and distal sites were measured at the preceding three time-points; analyses of radiographs were conducted by two investigators who did not participate in this study. The maximum MBL of the implant at each time-point was obtained as the corresponding MBL level. According to the T3 MBL level, all subjects were divided into two groups:

-Normal controls: less than 2 mm MBL in the first year after fixed prosthesis, then less than 0.2 mm MBL per year, or less than 0.017 mm per month

-Abnormal cases: MBL level exceeding normal controls

Finally, 41 abnormal cases and 40 normal controls were enrolled in the present study. The clinical variables of subjects were listed in Table 1.

2.3. Measurement of peri-implant bone morphological parameters

The second time-point radiographs were imported to CT Analyzer (Vision:1.8.1.3, SkyScan, Antwerpen, Belgium). Grayscale selection of radiographs was identified by screening out the high-density area as completely as possible (Fig. 1a). We confirmed the region of interest (ROI) by the diameter of each implant. Five sequential ROI layers adjoining the implant root were selected as the volume of interest (VOI) of peri-implant (Fig. 1b). Another five sequential ROI layers away from the implant were chosen as VOI of the normal adjacent (Fig. 1b). The trabecular bone morphological parameters, such as SMI, Tb.Pf, percent bone volume (BV/TV), intersection surface (i.S), and trabecular number (Tb.N) were extracted using three-dimensional analysis of each VOI. Finally, each morphological variable was calculated by the ratio of peri-implant to normal adjacent. The comparison of trabecular microarchitecture variables of subjects was exhibited in Table 2.

2.4. Visualization of correlation and covariance matrices

Correlation and covariance matrices can visualize the patterns and relationships between the variables. We had twenty original variables including object variable MBL. The visualization of matrices re-ordered the variables in a correlation matrix and displayed the value by sign and magnitude. All iconic encodings in the matrix displayed the pattern and significance level of correlations between variables. The R package corrgram and Hmisc were employed in this study.

2.5. Machine learning methods

Based on the R Programming Language (R Core Team, Vienna, Austria, 2016), four machine learning models, including Support vector machine (SVM), artificial neural network (ANN), logistic regression (LR) model and random forest (RF), were constructed. Their predictive performances and conventional parameters were compared. Seventy percent of samples were obtained as the training set for machine learning prediction models. The rest samples were used as the test set. LR model established with

variable choice through backward elimination was implemented to assess risk factors and predict the diagnosis of diseases. The R package e1071 was applied in the SVM model to accomplish regression and classification missions by constructing hyperplanes in a multidimensional space. SVM model could manage multiple continuous and categorical variables according to the decision plane. ANN model, a computerized encoding of artificial humanoid neuronal networks, included the input layer, hidden layers and output layer. Neurons connected the adjacent layers as a medium for the delivery-feedback-correction-delivery cycle. This recursive process adjusted the weights for less errors and better accuracy. ANN model was implemented by R package neural net. RF model, a machine learning algorithm based on the decision tree, could combine the output of a single decision tree to improve the overall performance. RF model was superior to a single decision tree in eliminating overfitting. RF model also could display the relative importance of the variables by the Gini index. The R package randomForest was utilized in the establishment of the RF model.

2.6. Statistical analysis

The chi-square test and Fisher's exact test were applied to compare the variables of the abnormal cases and normal controls. The Cochran-Armitage trend test was utilized for categorical variables, while continuous variables were assessed by Student's t-test and the Mann-Whitney rank-sum test. R programming language was used for all statistical analyses, while $p < 0.05$ was regarded as statistically significant.

3. Results

3.1. Trabecular microarchitecture changes in abnormal cases

Each morphological parameter of the peri-implant and the normal adjacent was compared between the abnormal cases and the normal controls, respectively. SMI (P=0.007) and Tb.Pf (P=0.017) significantly increased in peri-implant of abnormal cases compared with the normal adjacent (Fig. 3). BV/TV (P=0.002), Tb.N (P=0.025), and I.S (P=0.030) significantly increased in peri-implant of normal controls compared with the normal adjacent (Fig. 2).

3.2. Correlation analysis of MBL

The logically obvious correlation between morphological parameters was shown in Figure 3, and almost all correlation coefficients reached remarkably significant levels (supplementary table 1). Meanwhile, the linearity and credibility of trabecular bone microparameters were verified. SMI (P=0.002) and Tb.Pf (P=0.0165) exhibited a significantly high positive correlation with MBL. However, BV/TV and bone surface volume ratio (BS/BV) manifested a negative correlation with MBL. Gender (P=0.007), cortical bone thickness (P=0.0072), and smoking (P=0.0079) were powerfully correlated with MBL.

3.3. Performance of machine learning models

Based on the consequence of correlation analysis, we eliminated some meaningless parameters to build accurate models. Each model was superior to a single predictor. The LR model performed the best (AUC = 0.956), followed by SVM (AUC = 0.928), RF (AUC = 0.917), ANN (AUC = 0.900), SMI alone (AUC = 0.705), Tb.Pf alone (AUC = 0.663), and BV/TV alone (AUC = 0.629) (Figure 4, Table 3). As the best model, the sensitivity and specificity of LR were 91.67% and 86.67% at its optimal cutoff, respectively. LR also presented a perfect optimal criterion (0.867), satisfied positive (0.846) and negative (0.929) predictive values, the maximum positive diagnose-likelihood-ratio (6.875), and the minimum negative diagnose-likelihood-ratio (0.096). Moreover, the LR model had the smallest false positivity and false negativity. The cutoff value of relative SMI was 1.027, while the corresponding sensitivity and specificity were 65.85% and 67.50%, respectively. The cutoff value of Tb.Pf relative value was 0.968, and the sensitivity and specificity were 63.41% and 62.50%, respectively. All parameters of each model were listed in Table 4. Based on the RF model, we rearranged the variables according to the importance of predicting MBL measurement through the Gini index (Fig. 5).

4. Discussion

Peri-implant marginal bone resorption is a common threat to long-term implant stability and success of implantation. Abnormally pathological MBL without effective treatment is often accompanied with peri-implant mucositis.[17] The previous research on MBL mainly concentrated on treatment, but the cause of MBL and the way to predict it has rarely been studied. Factors such as trabecular bone microstructure parameters that possibly affect MBL during bone remolding were known to us, but the role of trabecular bone in this progression was still unclear. In this study, we analyzed morphological parameters of trabecular bone in patients with MBL during bone remolding by CBCT scan and CT Analyzer analysis. Our results demonstrated the differences and correlations of morphological parameters between the controls and abnormal MBL cases during bone remolding.

Trabecular bone is a defining factor for quality of bones structured with a trabecular pattern.[18] Trabecular microarchitecture can be displayed by several morphological parameters, including BV/TV, i.S, Tb.Pf, SMI, Tb.Th and Tb.N. In the present study, during the early stage of functional loading, CBCT analysis exhibited a significant increase of SMI and Tb.Pf in abnormal cases, while BV/TV, i.S, and Tb.N increased in normal controls. This finding revealed that severe MBL was accompanied with inferior trabecular microarchitecture at the early post-loading stage, while normal MBL showed an increased bone mass. A previous study reported a similar trend: the preservation and improvement of trabecular microarchitecture always brought about a better therapeutic benefit for osteoporosis at multiple skeletal sites.[19] Our result indicated SMI, Tb.Pf, BV/TV, i.S, and Tb.N at the early stage could be predictors for MBL level in the later stage, which was inconsistent with the previous studies in which bone remolding was believed to be closely associated with implant prognosis.[20]

Inspired by the above findings, we analyzed all variables using correlation and covariance matrices. All results relevant to morphological variables were confirmed with a significant difference and reasonable collinearity. Among them, SMI, Tb.Pf, Tb.N, BS/BV, and BV/TV manifested a higher correlation with MBL,

while other morphological variables could not bring a noteworthy contribution. These findings revealed that SMI and Tb.Pf were the best determinants of the MBL level. Both of them could reflect the structure quality of the trabecular bone and gained a decline in peri-implant of abnormal cases. However, Tb.N and BV/TV in normal controls were superior to other morphological variables, which accorded with the previous research.[20]

Accurate prediction of abnormally severe MBL at an early stage can aid in seeking possible factors that can influence normal bone remolding and prevent implant failure. Previous studies attempted to evaluate the risk of MBL using the proportion of cancellous bone,[11] crown-to-implant ratio,[21] bone texture and cortical width,[22] respectively. However, a single predictive factor may insufficient to accurately predict MBL occurrence, because MBL is a multifactorial outcome. As mentioned before, various factors, including cortical bone thickness, smoking, periodontitis, SMI, Tb.Pf, and BV/TV, might be regarded together as a complex to predict MBL.

Utilizing machine learning algorithms to predict the occurrence of MBL, the current study has obtained satisfying manifestation. An accurate prediction can warn patients and clinicians of possible factors that impact bone remolding, so as to intervene and avoid MBL timely.

A crucial finding that we extracted from the overall results is that the abnormal rise of SMI is tightly connected with severe MBL. Under proper stress, both osteocytes and osteoblasts, as effector cells of mechanical stimulation, can enhance bone formation and strength via a series of complex regulations.[23, 24] After bone remolding, the microdamage and repairment of the trabecular bone may typically achieve a dynamical balance.[25] However, the inferior trabecular structure model reveals that this balance is broken. If we find the detrimental factor that threatens the balance at an early stage and take intervention, severe MBL and implant failure may possibly be prevented, which is also the original intention of our research.

This study was restricted to patients receiving implant treatment in mandible. Mandible has thicker alveolar crest cortical bone than the maxilla.[26] Meanwhile, the maxilla implant is commonly in conjunction with bone augmentation. Previous predictive machine learning models had similar sample sizes in disease prediction.[16, 27, 28] Adding implant occlusion-related variables, such as overbite, overjet, median line location, or molar relationship, may enable better performing models based on the factors related to stress concentration. The current models all achieved considerable accuracy without incorporating the above variables, which was interesting. Due to the limited number of applicable subjects, we entitled this study as a preliminary one.

5. Conclusion

The current study verified that the severity of MBL was closely correlated to trabecular microarchitecture variance at the early stage of functional loading. This finding can provide an early warning for severe MBL. Machine learning models LR, SVM, RF, and ANN manifest superior performance compared to the single predictor in predicting peri-implant MBL in mandibula.

List Of Abbreviations

MBL
marginal bone loss
CBCT
cone-beam computed tomography
SVM
Support vector machine
ANN
artificial neural network
LR
logistic regression
RF
random forest
SMI
structure model index
Tb.Pf
trabecular pattern factor
ROI
region of interest
VOI
volume of interest
BV/TV
percent bone volume
i.S
intersection surface
Tb.N
trabecular number
BS/BV
bone surface volume ratio

Declarations

Ethics approval and consent to participate

This study was approved by the Ethical Committee of The Affiliated Stomatological Hospital of Nanjing Medical University (Approval number: PJ2019-038-001). According to the ethical standards, all patients provided written informed consent.

Consent for publication

Not applicable.

Availability of data and materials

The analyzed data sets generated during the study are available from the corresponding author on reasonable request.

Competing Interests

The authors declare that they have no competing interests.

Funding

This work was supported by the National Natural Science Foundation of China Grant (81771092), a project funded by the Priority Academic Program Development of Jiangsu Higher Education Institutions (PAPD, 2018-87), and Postgraduate Research & Practice Innovation Program of Jiangsu Province (KYCX19_1149).

Author contributions

The study was designed by HZ and HJ. The data was collected by HZ and analysed by JS. The paper was written by HZ and revised by JS, PZ, and HJ. They all made great contributions to this study and should be listed as authors. All authors read and approved the manuscript.

Acknowledgments:

Not applicable.

References

1. Esposito M, Hirsch JM, Lekholm U, Thomsen P: **Biological factors contributing to failures of osseointegrated oral implants. (I). Success criteria and epidemiology**. *Eur J Oral Sci* 1998, **106**(1):527-551.
2. Esposito M, Hirsch JM, Lekholm U, Thomsen P: **Biological factors contributing to failures of osseointegrated oral implants. (II). Etiopathogenesis**. *Eur J Oral Sci* 1998, **106**(3):721-764.
3. Albrektsson T, Zarb G, Worthington P, Eriksson AR: **The long-term efficacy of currently used dental implants: a review and proposed criteria of success**. *Int J Oral Maxillofac Implants* 1986, **1**(1):11-25.
4. Duan XB, Wu TX, Guo YC, Zhou XD, Lei YL, Xu X, Mo AC, Wang YY, Yuan Q: **Marginal bone loss around non-submerged implants is associated with salivary microbiome during bone healing**. *Int J Oral Sci* 2017, **9**(2):95-103.
5. Misch CE, Perel ML, Wang HL, Sammartino G, Galindo-Moreno P, Trisi P, Steigmann M, Rebaudi A, Palti A, Pikos MA *et al*: **Implant success, survival, and failure: the International Congress of Oral Implantologists (ICOI) Pisa Consensus Conference**. *Implant Dent* 2008, **17**(1):5-15.

6. Papaspyridakos P, Chen CJ, Singh M, Weber HP, Gallucci GO: **Success criteria in implant dentistry: a systematic review**. *J Dent Res* 2012, **91**(3):242-248.
7. Brägger U, Häfeli U, Huber B, Hämmerle CH, Lang NP: **Evaluation of postsurgical crestal bone levels adjacent to non-submerged dental implants**. *Clin Oral Implants Res* 1998, **9**(4):218-224.
8. Rho JY, Roy ME, Tsui TY, Pharr GM: **Elastic properties of microstructural components of human bone tissue as measured by nanoindentation**. *J Biomed Mater Res* 1999, **45**(1):48-54.
9. Zechner W, Trinkl N, Watzak G, Busenlechner D, Tepper G, Haas R, Watzek G: **Radiologic follow-up of peri-implant bone loss around machine-surfaced and rough-surfaced interforaminal implants in the mandible functionally loaded for 3 to 7 years**. *Int J Oral Maxillofac Implants* 2004, **19**(2):216-221.
10. Sener-Yamaner ID, Yamaner G, Sertgoz A, Canakci CF, Ozcan M: **Marginal Bone Loss Around Early-Loaded SLA and SLActive Implants: Radiological Follow-Up Evaluation Up to 6.5 Years**. *Implant Dent* 2017, **26**(4):592-599.
11. Simons WF, De Smit M, Duyck J, Coucke W, Quirynen M: **The proportion of cancellous bone as predictive factor for early marginal bone loss around implants in the posterior part of the mandible**. *Clin Oral Implants Res* 2015, **26**(9):1051-1059.
12. Corcuera-Flores JR, Alonso-Dominguez AM, Serrera-Figallo MA, Torres-Lagares D, Castellanos-Cosano L, Machuca-Portillo G: **Relationship Between Osteoporosis and Marginal Bone Loss in Osseointegrated Implants: A 2-Year Retrospective Study**. *J Periodontol* 2016, **87**(1):14-20.
13. Levin L, Hertzberg R, Har-Nes S, Schwartz-Arad D: **Long-term marginal bone loss around single dental implants affected by current and past smoking habits**. *Implant Dent* 2008, **17**(4):422-429.
14. Cruz JA, Wishart DS: **Applications of machine learning in cancer prediction and prognosis**. *Cancer Inform* 2007, **2**():59-77.
15. Kourou K, Exarchos TP, Exarchos KP, Karamouzis MV, Fotiadis DI: **Machine learning applications in cancer prognosis and prediction**. *Comput Struct Biotechnol J* 2015, **13**:8-17.
16. Kim DW, Kim H, Nam W, Kim HJ, Cha IH: **Machine learning to predict the occurrence of bisphosphonate-related osteonecrosis of the jaw associated with dental extraction: A preliminary report**. *Bone* 2018, **116**:207-214.
17. Heitz-Mayfield LJA, Salvi GE: **Peri-implant mucositis**. *J Clin Periodontol* 2018, **45 Suppl 20**:S237-S245.
18. Ribeiro-Rotta RF, Lindh C, Rohlin M: **Efficacy of clinical methods to assess jawbone tissue prior to and during endosseous dental implant placement: a systematic literature review**. *Int J Oral Maxillofac Implants* 2007, **22**(2):289-300.
19. Chesnut CH, 3rd, Majumdar S, Newitt DC, Shields A, Van Pelt J, Laschansky E, Azria M, Kriegman A, Olson M, Eriksen EF *et al*: **Effects of salmon calcitonin on trabecular microarchitecture as determined by magnetic resonance imaging: results from the QUEST study**. *J Bone Miner Res* 2005, **20**(9):1548-1561.
20. Maquer G, Musy SN, Wandel J, Gross T, Zysset PK: **Bone volume fraction and fabric anisotropy are better determinants of trabecular bone stiffness than other morphological variables**. *J Bone Miner*

Res 2015, **30**(6):1000-1008.

21. Di Fiore A, Vigolo P, Sivolella S, Cavallin F, Katsoulis J, Monaco C, Stellini E: **Influence of Crown-to-Implant Ratio on Long-Term Marginal Bone Loss Around Short Implants**. *Int J Oral Maxillofac Implants* 2019, **34**(4):992-998.
22. Merheb J, Graham J, Coucke W, Roberts M, Quirynen M, Jacobs R, Devlin H: **Prediction of implant loss and marginal bone loss by analysis of dental panoramic radiographs**. *Int J Oral Maxillofac Implants* 2015, **30**(2):372-377.
23. Morrell AE, Brown GN, Robinson ST, Sattler RL, Baik AD, Zhen G, Cao X, Bonewald LF, Jin W, Kam LC *et al*: **Mechanically induced Ca(2+) oscillations in osteocytes release extracellular vesicles and enhance bone formation**. *Bone Res* 2018, **6**:6.
24. Wang C, Shan S, Wang C, Wang J, Li J, Hu G, Dai K, Li Q, Zhang X: **Mechanical stimulation promote the osteogenic differentiation of bone marrow stromal cells through epigenetic regulation of Sonic Hedgehog**. *Exp Cell Res* 2017, **352**(2):346-356.
25. Nagaraja S, Couse TL, Guldberg RE: **Trabecular bone microdamage and microstructural stresses under uniaxial compression**. *J Biomech* 2005, **38**(4):707-716.
26. Coskun I, Kaya B: **Relationship between alveolar bone thickness, tooth root morphology, and sagittal skeletal pattern : A cone beam computed tomography study**. *J Orofac Orthop* 2019, **80**(3):144-158.
27. Shipp MA, Ross KN, Tamayo P, Weng AP, Kutok JL, Aguiar RC, Gaasenbeek M, Angelo M, Reich M, Pinkus GS *et al*: **Diffuse large B-cell lymphoma outcome prediction by gene-expression profiling and supervised machine learning**. *Nat Med* 2002, **8**(1):68-74.
28. Lee H, Shin SY, Seo M, Nam GB, Joo S: **Prediction of Ventricular Tachycardia One Hour before Occurrence Using Artificial Neural Networks**. *Sci Rep* 2016, **6**:32390.

Tables

Table 1 Comparison of variables between abnormal cases and normal controls.

Marginal bone loss	Normal control (n = 40)	Abnormal case (n = 41)	*P*-value
Age (year)			0.307
Mean ± sd	60.9 ± 10.7	58.2 ± 13.0	
Median [IQR]	59.0 [55.0; 71.8]	59.0 [49.0; 70.0]	
Gender			0.007**
Female	9	21	
Male	31	20	
Periodontitis			0.291
Yes	13	18	
No	27	23	
Implant Diameter (mm)			0.404
≤4	13	17	
>4	27	24	
Implant Length (mm)			0.967
≤8	5	5	
>8	35	36	
Implant Area			0.376
Anterior region	12	7	
Premolar area	5	7	
Molar area	23	27	
Retention selection			0.315
Screw retention	23	28	
Adhesive retention	17	13	
Cortical bone thickness (mm)			0.007**
Mean ± sd	1.25 ± 0.32	1.48 ± 0.43	
Median [IQR]	1.21 [1.04; 1.40]	1.41 [1.15; 1.83]	
Smoking			0.008**
Yes	30	19	
No	10	22	
Time-point 2 (month)			0.031*
Mean ± sd	4.2 ± 1.1	3.8 ± 1.0	
Median [IQR]	4.0 [3.1; 5.0]	3.5 [3.0; 4.5]	
Time-point 3 (month)			< 0.001***
Mean ± sd	20.2 ± 1.7	21.7 ± 3.2	
Median [IQR]	20.0 [19.0; 21.8]	23.0 [20.0; 24.0]	
Time-point 2 MBL (mm)			0.006**
Mean ± sd	0.78 ± 0.05	0.81 ± 0.04	
Median [IQR]	0.78 [0.71; 0.82]	0.81 [0.78; 0.83]	
Time-point 3 MBL (mm)			< 0.001***
Mean ± sd	1.44 ± 0.32	2.97 ± 0.58	
Median [IQR]	1.45 [1.26; 1.72]	2.90 [2.52; 3.35]	

Abbreviations; sd: standard deviation, IQR: Interquartile range

* $p < 0.05$, ** $p < 0.01$, *** $p < 0.001$

Table 2 Comparison of trabecular microarchitecture between abnormal cases and normal controls

Marginal bone loss	Normal control (n = 40)	Abnormal case (n = 41)	*P*-value
Percent bone volume, BV/TV			0.045*
Mean ± sd	1.08 ± 0.24	0.96 ± 0.36	
Median [IQR]	1.08 [1.00; 1.15]	0.99 [0.80; 1.14]	
Bone surface, BS			0.098
Mean ± sd	1.03 ± 0.18	0.96 ± 0.23	
Median [IQR]	1.02 [0.96; 1.09]	0.97 [0.90; 1.05]	
Intersection surface, i.S			0.113
Mean ± sd	1.10± 0.33	0.99 ± 0.46	
Median [IQR]	1.11 [0.95; 1.19]	0.98 [0.77; 1.24]	
Bone surface/volume ratio, BS/BV			0.23
Mean ± sd	0.98 ± 0.18	1.12 ± 0.45	
Median [IQR]	0.95 [0.88; 1.07]	1.02 [0.83; 1.23]	
Bone surface density, BS/TV			0.082
Mean ± sd	1.03 ± 0.18	0.94 ± 0.21	
Median [IQR]	1.02 [0.96; 1.09]	0.97 [0.90; 1.05]	
Trabecular pattern factor, Tb.Pf			0.012*
Mean ± sd	1.00 ± 0.48	1.29 ± 0.58	
Median [IQR]	0.90 [0.73; 1.16]	1.14 [0.89; 1.64]	
Structure model index, SMI			0.001**
Mean ± sd	0.96 ± 0.22	1.14 ± 0.25	
Median [IQR]	0.95 [0.82; 1.07]	1.09 [0.96; 1.29]	
Trabecular thickness, Tb.Th			0.59
Mean ± sd	1.01 ± 0.17	1.01 ± 0.24	
Median [IQR]	1.01 [0.93; 1.10]	0.99 [0.84; 1.18]	
Trabecular number, Tb.N			0.008**
Mean ± sd	1.06 ± 0.20	0.93 ± 0.26	
Median [IQR]	1.05 [0.97; 1.14]	0.97 [0.83; 1.07]	
Trabecular separation, Tb.Sp			0.713
Mean ± sd	1.00 ± 0.05	1.01 ± 0.06	
Median [IQR]	1.00 [0.97; 1.02]	1.00 [0.97; 1.02]	

Abbreviations; sd: standard deviation, IQR: Interquartile range

* $p < 0.05$, ** $p < 0.01$, *** $p < 0.001$

Table 3 Statistical significance of the difference between the areas under ROC curves. DeLong's test and Bootstrap test were used.

	SVM	RF	ANN	SMI alone	Tb.Pf alone	BV/TV alone
	P-value	*P*-value	*P*-value	*P*-value	*P*-value	*P*-value
egression (LR)	0.263	0.182	0.152	0.000***	0.000***	0.000***
ector machine		0.435	0.346	0.001**	0.000***	0.999
orest (RF)			0.356	0.005**	0.001**	0.000***
neural network				0.019*	0.007**	0.002**
e					0.169	0.162
ne						0.345

* $p < 0.05$, ** $p < 0.01$, *** $p < 0.001$

Table 4 Sensitivity, specificity and other conventional parameters of each model at optimal cutoff point

y	specificity	Optimal cutoff of probability	Positive Predictive Value	Negative Predictive Value	DLR Positive	DLR Negative	False positive	False negative	Optimal criterion
	86.7%	0.644	0.846	0.929	6.875	0.096	2	1	0.867
	83.3%	0.539	0.857	0.769	4.800	0.240	2	3	0.800
	80.0%	0.526	0.769	0.857	4.167	0.208	3	2	0.800
	93.3%	0.854	0.909	0.875	12.500	0.179	1	2	0.833
	67.5%	1.027	0.675	0.659	2.026	0.506	13	14	0.659
	62.5%	0.968	0.634	0.625	1.691	0.585	15	15	0.625
	45.0%	1.049	0.421	0.419	0.710	1.355	22	25	0.390

Optimal cutoff was considered as the point maximizing the sum of sensitivity and specificity.

Figures

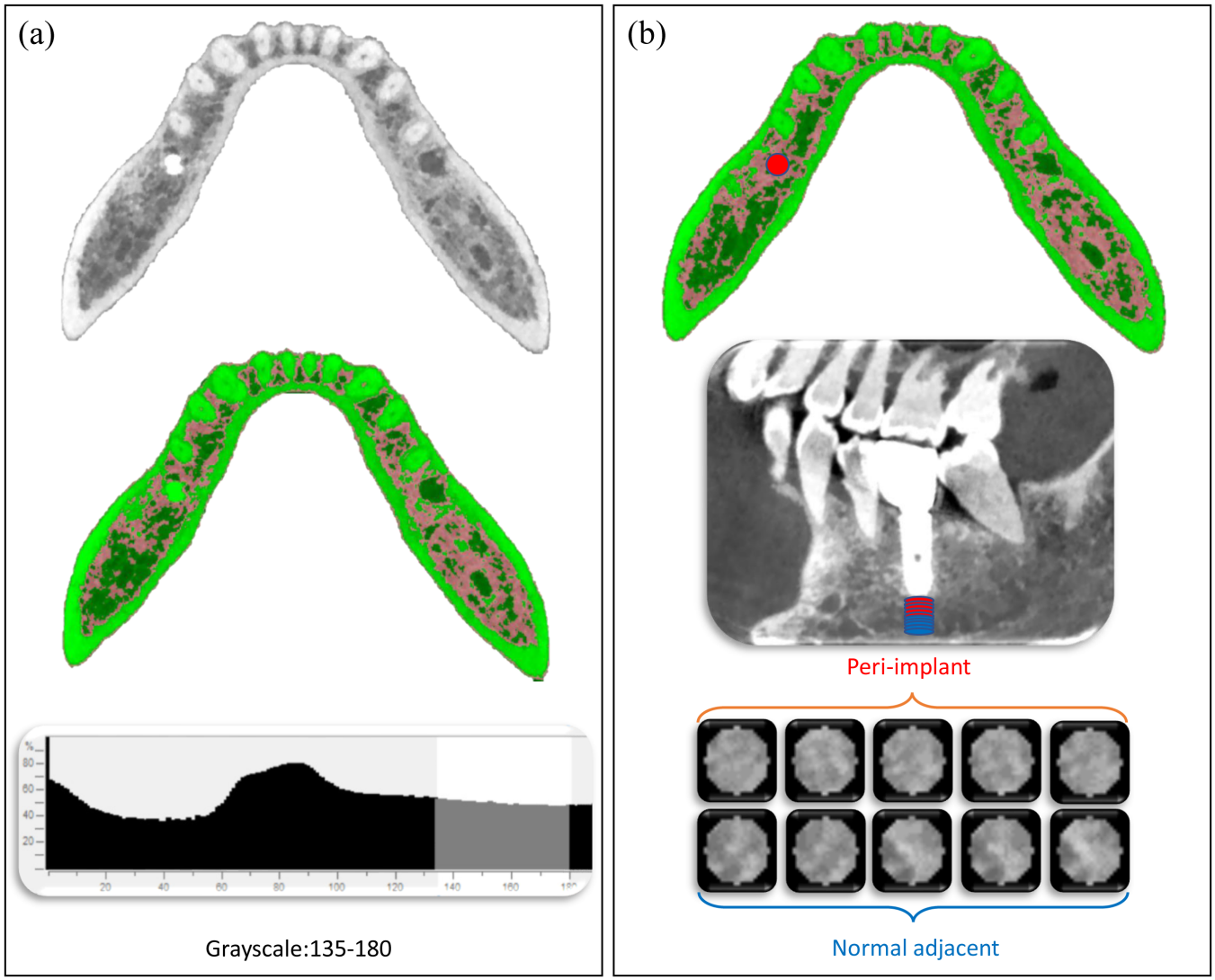

Figure 1

Measurement of peri-implant bone morphological parameters. (a) Radiograph grayscale was selected by the principle of showing trabecular bone (marked in red) completely. (b) Five sequential ROI layers adjoining the implant were selected as VOI of peri-implant (marked in red). Five sequential ROI layers away from implant were chosen as VOI of the normal adjacent (marked in blue).

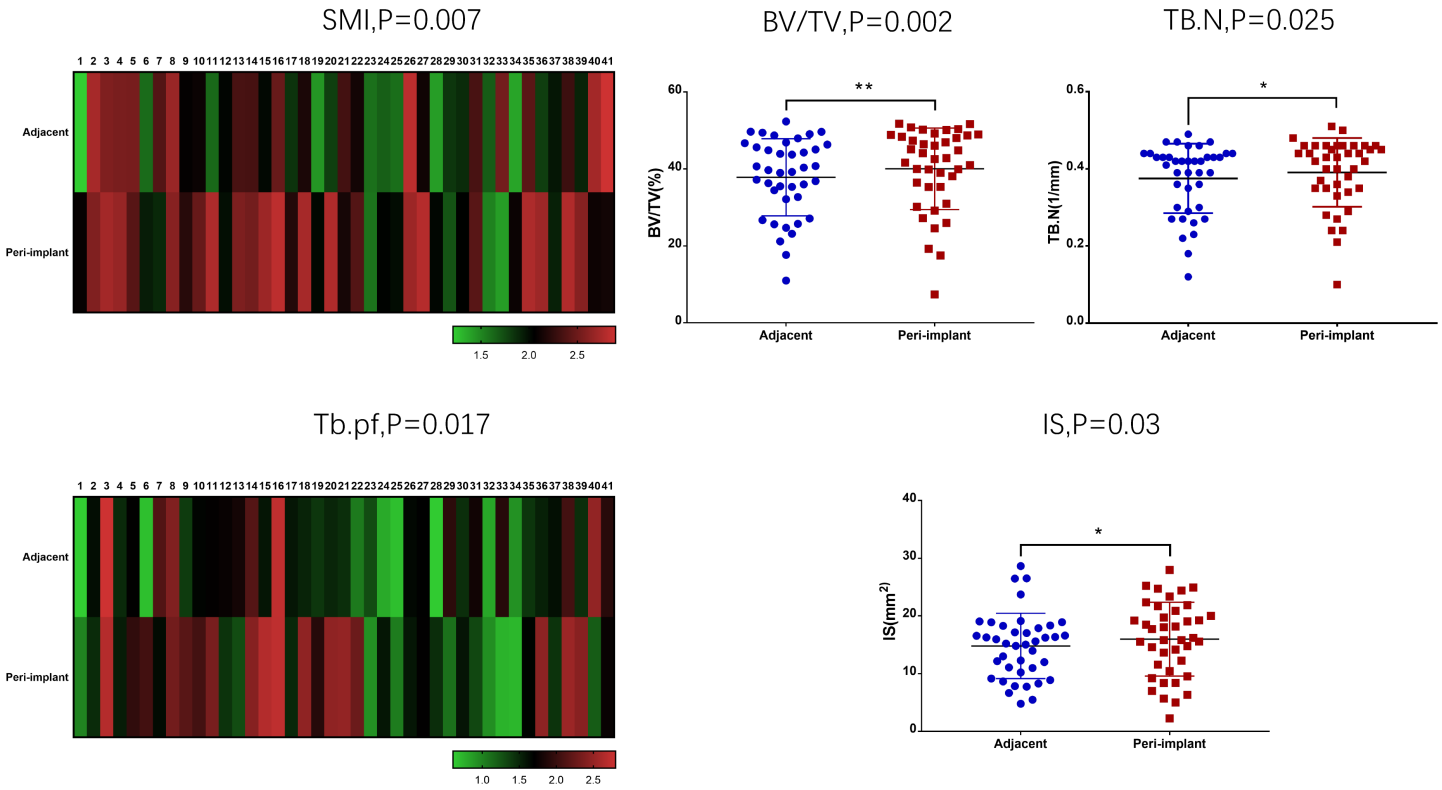

Figure 2

Comparison of morphological parameters among peri-implant and normal adjacent in cases and controls. In severe MBL cases, SMI and Tb.Pf showed visible difference between peri-implant and adjacent. BV/TV, Tb.N and i.S exhibited significant difference between peri-implant and adjacent in normal controls.

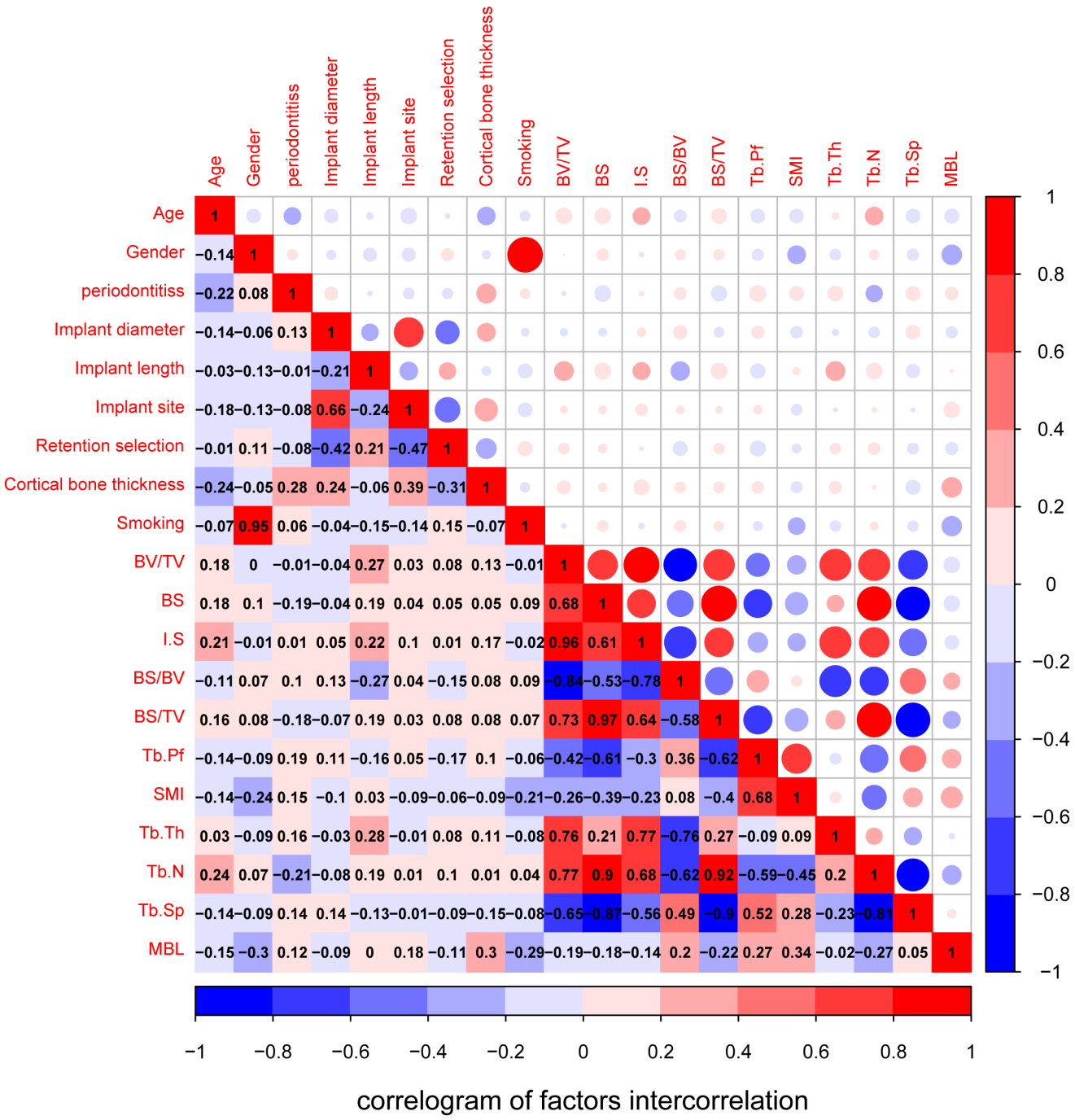

Figure 3

The visualization of correlation and covariance matrices between all variables. Red and blue represent positive and negative correlation respectively. Darker colors indicate greater correlation.

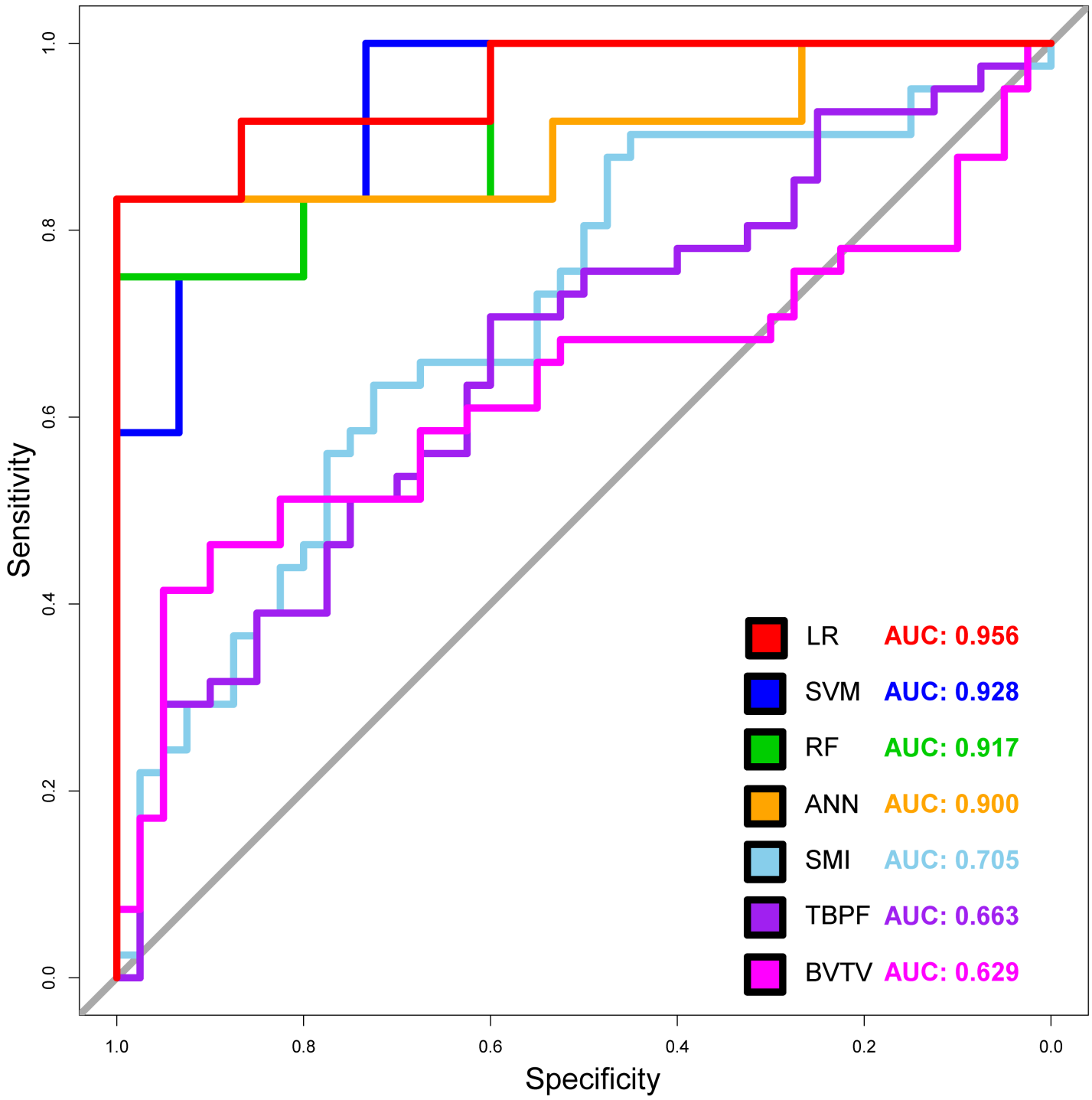

Figure 4

ROC & AUC of prediction models. Sensitivity and specificity of LR, the best performing model, were 91.7% and 86.7%, respectively at its optimal cutoff.

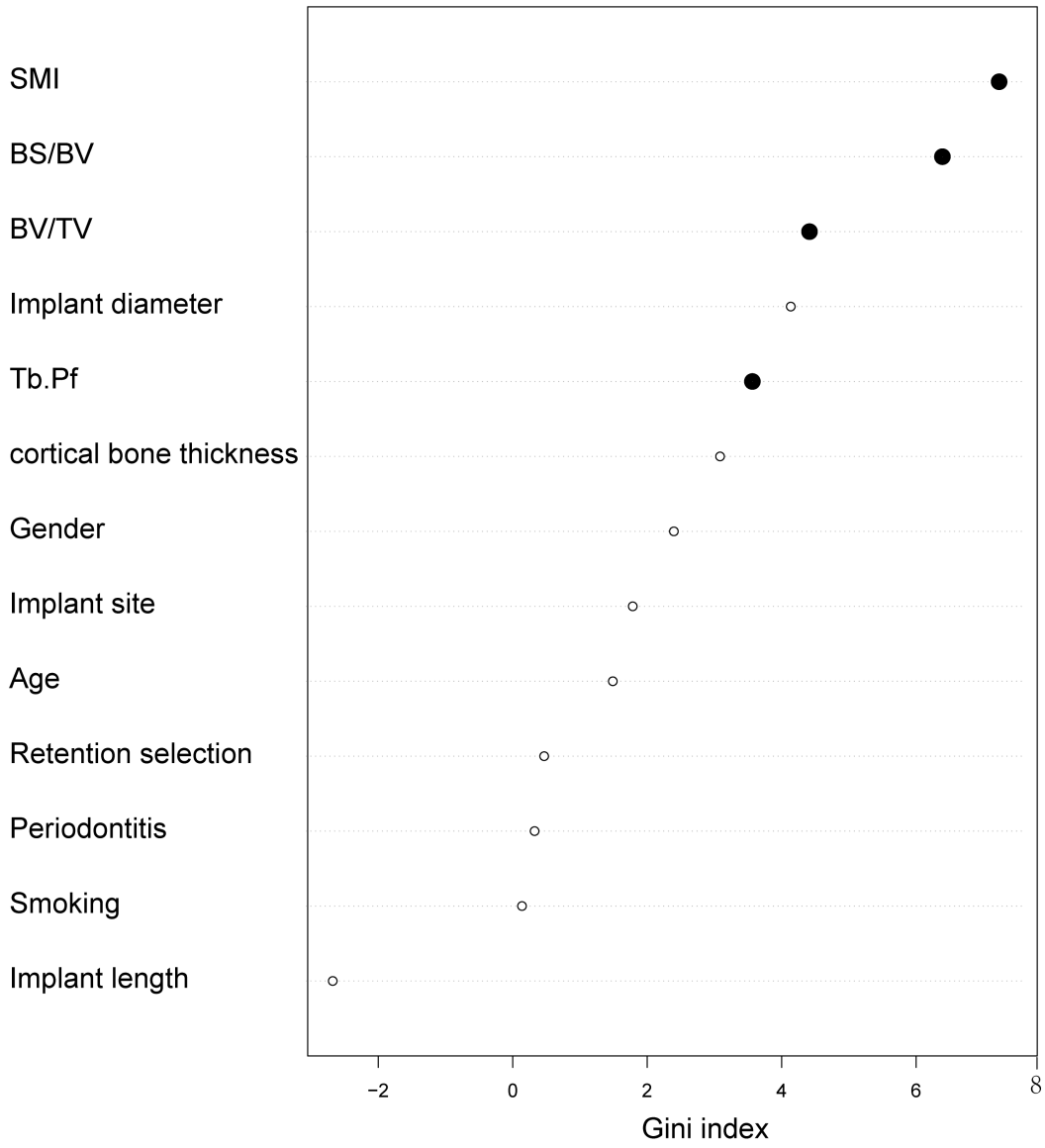

Figure 5

Variable importance plot of random forest model. The plot indicates relative importance of the variables in random forest model. Gini index reflects the reduction in entropy. An attribute with a higher value should be placed as root and a branch with 0 entropy should be converted to a leaf node. A branch with entropy higher than 0 needs further splitting. Trabecular microarchitecture variables are marked as solid black points.

Supplementary Files

This is a list of supplementary files associated with this preprint. Click to download.

- SupplementaryTable1.xlsx